www.ietdl.org

Published in IET Optoelectronics
Received on 15th May 2013
Revised on 1st September 2013
Accepted on 9th October 2013
doi: 10.1049/iet-opt.2013.0044

Special Issue on Semiconductor Lasers and Integrated Optoelectronics

ISSN 1751-8768

Simulated dynamics of optically pumped dilute nitride 1300 nm spin vertical-cavity surface-emitting lasers

Sami S. Alharthi, Rihab K. Al Seyab, Ian D. Henning, Michael J. Adams

School of Computer Science and Electronic Engineering, University of Essex, Wivenhoe Park, Colchester CO4 3SQ, UK
E-mail: ssmalh@essex.ac.uk

Abstract: The authors report a theoretical analysis of optically pumped 1300 nm dilute nitride spin-polarised vertical-cavity surface-emitting lasers (VCSELs) using the spin-flip model to determine the regions of stability and instability. The dependence of the output polarisation ellipticity on that of the pump is investigated, and the results are presented in two-dimensional contour maps of the pump polarisation against the magnitude of the optical pump. Rich dynamics and various forms of oscillatory behaviour causing self-sustained oscillations in the polarisation of the spin-VCSEL subject to continuous-wave pumping have been found because of the competition of the spin-flip processes and birefringence. The authors also reveal the importance of considering both the birefringence rate and the linewidth enhancement factor when engineering a device for high-frequency applications. A very good agreement is found with the experimental results reported by the authors' group.

1 Introduction

Research on spin-polarised lasers is relatively new within optoelectronics, and the recent demonstrations of the spin-polarised light-emitting diodes and vertical-cavity surface-emitting lasers (VCSELs) [1] represent the first ground-breaking steps in spin optoelectronics. Owing to their possibilities for non-linear responses, spin-controlled light sources have the potential to spawn new applications in optical information processing and data storage, optical communication, optical amplification, quantum computing and biochemical sensing (including chiral spectroscopy) [2]. Spin-VCSELs offer the attractive prospect of output polarisation control through the injection of spin-polarised electrons. A spin-polarised electron population can be achieved via either an electrical injection using magnetic contacts or by optical pumping using circularly polarised light.

Recent research advances in this area have included the demonstrations of an electrically injected quantum dot spin-VCSEL [3] and an optically pumped spin-VCSEL grown on a (110) substrate to achieve a high degree of circular polarisation associated with an enhanced spin lifetime [4]. Very recently, the first continuous-wave optically pumped dilute nitride spin-VCSEL operating at 1300 nm with output polarisation determined by that of the pump has been reported [5] and the same structure also yielded the first self-sustained periodic oscillations, tunable from 8.6 to 11 GHz with the pump polarisation [6]. Controlling the output polarisation by that of the input is experimentally demonstrated in [7–9]. Also, transient oscillations of the output ellipticity in response to pulsed optically spin-polarised pumping were predicted and observed in [10–12] and were reported for conventional electrical pumping in [13, 14]. Simulations using the spin-flip model (SFM) yielded good agreement with these experimental results, confirming that the oscillation frequency is dominated by the birefringence of the microcavity in combination with the dichroism and the spin relaxation rate, as originally predicted by Gahl *et al.* [15]. In the present contribution, the SFM is used to predict the more general dependence of the spin-VCSEL output power and the polarisation on the pump power and the polarisation for the 1300 nm dilute nitride structures.

The demonstrated optically pumped dilute nitride VCSEL [16] is a promising candidate for an optically pumped spin-VCSEL. The combination of the GaInNAs/GaAs active regions with the GaAs/AlAs distributed Bragg reflectors (DBRs) is an attractive system for the 1.3 μm VCSEL devices [16]. In the devices designed to operate under optical pumping, it has been shown experimentally that even small concentrations of nitrogen in the active material lead to a significant increase of the spin relaxation time because of the formation of defects which slow down the dominant D'yakonov–Perel room temperature spin-relaxation mechanism [17, 18].

2 Theoretical model

The four-level (SFM) derived first by San Miguel *et al.* in 1995 [19] and developed further in [15, 20] was used to investigate the characteristics and the stability of the optically pumped 1300 nm dilute nitride GaInNAs spin-VCSELs. The SFM rate equations are written in terms of right- and left-circularly polarised complex fields denoted by $\bar{E}_+$ and $\bar{E}_-$, respectively, with the corresponding normalised carrier densities n_+ and n_- associated with the

spin-down and the spin-up electron populations, respectively. In the present contribution, we follow the same approach reported in [15, 21, 22] to treat and solve the SFM rate equations.

Numerical solutions for the full set of the SFM rate equations provide a time series for the output power of the circularly polarised intensities $I_+ = |E_+|^2$ and $I_- = |E_-|^2$ in addition to the corresponding normalised carrier densities $N = (n_+ + n_-)/2$ and $m = (n_+ - n_-)/2$. These solutions can be presented as two-dimensional (2D) contour maps in the plane of the normalised pump power $\eta = \eta_+ + \eta_-$, where η_+ and η_- are the right- and the left-circularly polarised normalised pump components and the pump polarisation ellipticity P is defined as

$$P = \frac{\eta_+ - \eta_-}{\eta_+ + \eta_-}$$

These maps represent the output in terms of the circularly polarised intensities I_+, I_-, $I_{\text{total}} = (I_+ + I_-)$, and the polarisation ellipticity (ε) is defined as

$$\varepsilon = \frac{|E_+|^2 - |E_-|^2}{|E_+|^2 + |E_-|^2}$$

These maps have been used to predict and simulate the more general characteristics and the stability behaviours for two samples of the optically pumped 1300 nm dilute nitride GaInNAs spin-VCSELs used recently at room temperature under CW pumping by our group [5, 6]. The experimental investigations on these spin-VCSELs showed different stability behaviours. For a stable behaviour, it has been demonstrated that the output polarisation ellipticity (ε) follows the one of the pump (P) as reported in [5]. Moreover, the polarisation oscillations have been observed in the range of 8.6–11 GHz under some conditions as reported in [6].

This motivates us to simulate and predict the observed behaviours and explore the influence of the SFM parameters.

3 Results and discussions

To see the whole picture of the dynamic behaviour of the 1300 nm GaInNAs spin-VCSELs, 2D contour maps in the plane of the pump power η and the pump polarisation P have been calculated for the two spin-VCSEL samples by using the SFM parameters as reported in [5, 6]. These parameters have been found by fitting the experimental data and they are summarised in Table 1.

3.1 Influence of the SFM parameters on 1300 nm GaInNAs spin-VCSEL sample 1

The steady-state values and the polarisation properties of the first sample of the 1300 nm dilute nitride ($Ga_{0.67}In_{0.33}N_{0.016}As_{0.984}$ QWs and $Ga_{0.75}In_{0.25}N_{0.017}As_{0.983}$ strain-mediating layers) spin-VCSEL have been calculated and presented as 2D contour maps in the plane of (η–P) for the normalised circularly polarised output intensities I_+, I_-, $I_{\text{total}} = (I_+ + I_-)$, and the polarisation ellipticity (ε) in Figs. 1*a*–*d* by using the same parameter set as summarised in Table 1 under sample 1 and reported in [5].

The simulated results demonstrate that the polarisation of the output of the optically pumped VCSEL can be controlled by the polarisation of the optical pump as can be seen in the contours in Fig. 1. This is in good agreement with the predicted results reported in [15] and with the experimental results demonstrated under the pulsed pumping in [7–9]. Colours in the map indicate the steady-state values of the normalised output intensities and the output polarisation ellipticity (ε) when the VCSEL is stable (see the colour bars for the values). It is clear from Figs. 1*a* and *b* that when the VCSEL is fed with a right $P = +1$ (left $P = -1$) circularly polarised pump, the right I_+ (left I_-) circularly polarised mode of the VCSEL appears as the dominant mode whereas the other mode I_- (I_+) is off. These two maps show that at a certain pump power when I_+ (I_-) is the dominant mode, its intensity decreases by reducing (increasing) the pump ellipticity from $P = +1$ to $P = -1$ ($P = -1$ to $P = +1$) and the reverse holds true for the non-lasing mode I_- (I_+). It is also noted from Fig. 1*b* (1*a*) that the threshold of the non-lasing mode I_- under the right circularly polarised pump $P = +1$ (I_+ under the left-circularly polarised pump $P = -1$) is delayed until about twice the threshold ($\eta = 2$) of the lasing mode. Fig. 1*c* indicates that the laser is stable and the total output intensity appears approximately independent of the pump ellipticity P with linear proportionality to the pump intensity η. In fact, the total intensity I_{total} is slightly

Table 1 SFM parameters for the two samples of the GaInNAs spin-VCSELs

Parameter	Description	Sample 1 [5]	Sample 2 [6]
α	linewidth enhancement factor	2	5
γ_p	birefringence rate	5 rad/ns	34.5 rad/ns
γ_s	spin relaxation rate	105 rad/ns	105 rad/ns
γ_a	gain anisotropy (dichroism)	0 GHz	0 GHz
γ	electron density decay rate	1 GHz	1 GHz
κ	photon decay rate	250 GHz	250 GHz

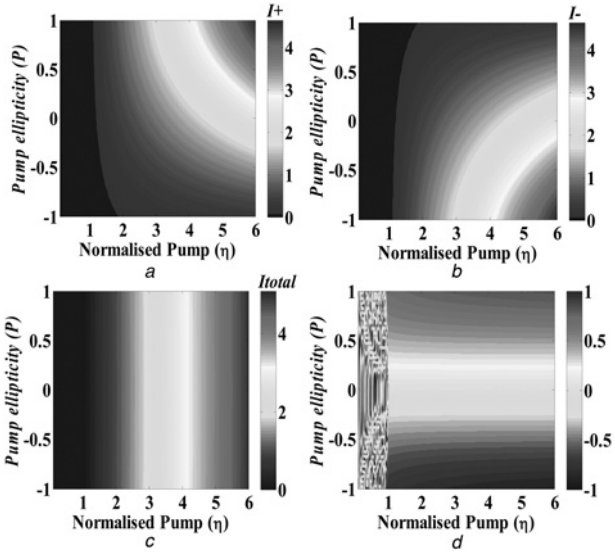

Fig. 1 *Calculated 2D contour maps for 1300 nm dilute nitride spin-VCSELs (sample 1) normalised output intensities*

a I_+
b I_-
c I_{total}
d and the output polarisation ellipticity ε using SFM parameters as in [5]

doi: 10.1049/iet-opt.2013.0044

affected by the pump polarisation when $|P| > 0.7$, but this effect is not noticeable on the scale of this map and would be much clearer in the output polarisation ellipticity (ε) map. The output polarisation ellipticity is presented in Fig. 1*d*. This contour demonstrates that the output polarisation elllipticity follows the one of the pump. The randomly coloured area in this map refers to the spontaneous emission below the threshold where the VCSEL is not lasing. It can be seen from this map that by increasing the pump power, the value of the output polarisation ellipticity (ε) increases then saturates and a high degree of output circular polarisation is achievable on this spin-VCSEL at high pump powers when $|P| = 1$. These simulation results show a very good agreement with the experimental results presented in [5].

3.2 Influence of the SFM parameters on 1300 nm GaInNAs spin-VCSEL sample 2

In this subsection, we present the same contour maps for the 1300 nm dilute nitride ($Ga_{0.71}In_{0.29}N_{0.020}As_{0.980}$ QWs and $Ga_{0.80}In_{0.20}N_{0.022}As_{0.978}$ strain-mediating layers) spin-VCSEL where polarisation oscillations have been observed in the experimental work. Figs. 2*a–d* shows the calculated contour maps for the variables I_+, I_-, I_{total} and the output polarisation ellipticity (ε) by using the SFM parameters summarised in Table 1 under sample 2 and reported in [6]. The coloured regions in the maps indicate the steady-state values of the normalised intensity and the output polarisation when the spin-VCSEL is stable whereas the white region indicates the region of instability where the spin-VCSEL is unstable and shows polarisation oscillations caused by the competition between the spin relaxation processes and the birefringence as first predicted theoretically in [15] and studied further in [21].

The contours in Fig. 2 show completely different shapes and behaviours from those simulated for sample 1. These differences arise from slight changes in the parameter values of the birefringence (γ_p) and the linewidth enhancement factor (α). The changes in the birefringence lead to changes in the frequency of the oscillations whereas the changes in the linewidth enhancement factor influence the amplitude of the oscillations. Variations in the birefringence and the α factor values are attributed to strain and the fundamental physical processes at work in the device [15]. It can be seen from Figs. 2*a* and *b* that the instability region widens with the increasing optical pump power until it becomes dominant beyond five times the threshold ($\eta > 5$) at all the polarisation values (P). It is also clear that the right (left) circularly polarised component I_+ (I_-) gives the highest intensity under the left (right) circularly polarised pump which is an indication of the polarisation switching (PS) as will be discussed later. Fig. 2*c* presents the total output intensity contour map and illustrates that the total output intensity increases with the increasing optical pump whereas it seems to be independent of the pump polarisation within the stable region.

In Fig. 2*d*, the output polarisation ellipitcity (ε) has been mapped in the plane of (η–P). This map shows that the output polarisation ellipticity (ε) of the dilute nitride spin-VCSEL is controlled by that of the pump within the stability region (the almost triangular golden yellow and indigo areas within the range $1 < \eta < 2$ and $0.25 < |P| < 1$). Outside this range and within the stability region, the spin-VCSEL switches to the opposite polarisation state (e.g. from right- to left-circular polarisation or the reverse) showing the PS. To see the PS clearly, the output polarisation ellipticity (ε) has been plotted against the pump ellipticity P at two pump powers, ($\eta = 1.5$ and $\eta = 4$, respectively, as indicated by the dashed lines in Fig. 2*d*), in Figs. 3*a* and *b*, respectively. To identify the polarisation selection mechanisms, it is necessary to determine the regions of stability and of the PS by performing a Routh–Hurwitz stability analysis; however, this is beyond the scope of the present paper.

Fig. 3*a* demonstrates that the output polarisation ellipticity (ε) follows that of the pump at the beginning and then it switches to the opposite state after passing through the instability region. Furthermore, Fig. 3*b* shows that a relatively high output polarisation degree (about 0.75) is achievable with a lesser degree of the pump polarisation (about 0.25). This feature offers polarisation amplification and the amplification of the spin information which are considered as the great advantages of the spin-VCSELs [1, 23].

The PS and the polarisation oscillations denoted by the white regions in Fig. 2 are caused by the competition

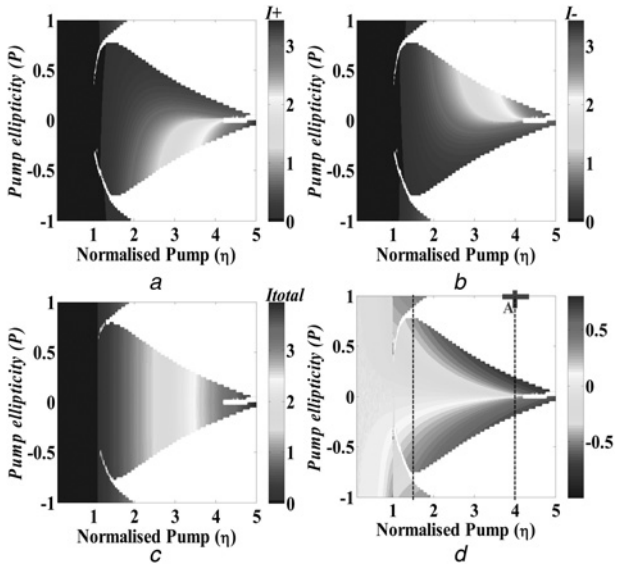

Fig. 2 *Calculated 2D contour maps for 1300 nm dilute nitride spin-VCSELs (sample 2) normalised output intensities*

a I_+
b I_-
c I_{total}
d and the output polarisation ellipticity ε using SFM parameters as in [6]

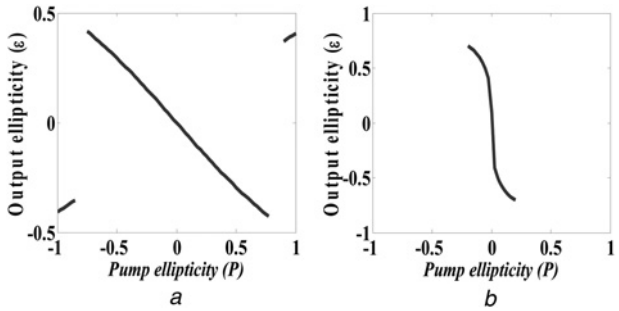

Fig. 3 *Spin-VCSEL (sample 2) output ellipticity as a function of the pump ellipticity at*

a $\eta = 1.5$
b $\eta = 4$

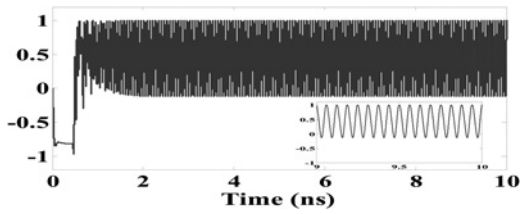

Fig. 4 *Calculated time series of the output polarisation ellipticity for sample 2 at ($\eta = 4$, $P = +1$)*

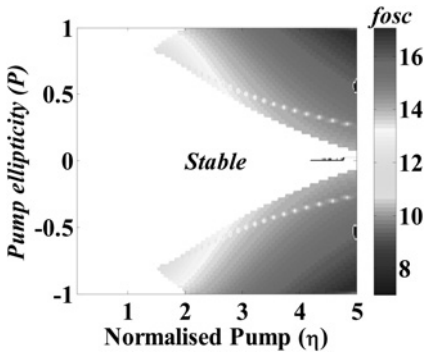

Fig. 5 *Calculated 2D contour map for the frequency of oscillation f_{osc} (in GHz) of the spin-VCSEL instabilites*

between the fundamental physical processes at work in the device, namely the spin-flip processes that tend to equalise the gain for the right- and the left-circularly polarised fields, the dichroism which tries to equalise the field amplitudes and the birefringence which couples power back and forth between the polarised fields [15]. Therefore special care should be taken when engineering a device for the high-frequency applications. These polarisation oscillations are related to PS and the development of the ellipticity in the case of $P = 0$ [13, 20, 24].

Now, we would like to investigate the instability region in more detail. For this task, the time series of the output polarisation ellipticity has been generated as in Fig. 4 for this sample at point A which represents the parameters ($\eta = 4$, $P = +1$). This figure demonstrates the oscillations of the polarisation of the emitted light. Moreover, if we zoom in on the last nanosecond of the time series, we can see that these polarisation oscillations form self-sustained periodic oscillations as illustrated in the inset. Such self-sustained polarisation oscillations are of interest for optical clock generation, especially since the frequency can be tuned with the pump polarisation.

To see the influence of the SFM parameters of sample 2 on the polarisation oscillation frequency, the fast Fourier transform has been used to transform the time series to the frequency domain. The frequency of oscillation (f_{osc}) for the instability region is presented in a 2D contour map in Fig. 5.

Fig. 5 illustrates that the frequency of oscillations is influenced by the variations in the pump power η and the pump ellipticity P (see the colour bar for values in Gigahertz). The frequency of the oscillations increases as the pump power increases. It is also sensitive to the pump ellipticity where it increases as the pump polarisation ellipticity P goes to a high degree of circular polarisation. These results show a very good agreement with the experimental results presented in [6], where polarisation oscillations have been observed in the range of 8.6–11 GHz. Transient oscillations around 10 GHz have been reported at shorter wavelengths at room temperature for the spin-VCSEL in [10–12].

4 Conclusion

In this paper, we presented the simulated dynamics for the 1300 nm dilute nitride spin-VCSELs under CW pump at room temperature. These dynamics have been modelled by using the SFM. Two sets of parameters have been used for two samples of 1300 nm dilute nitride spin-VCSEL. The simulated results demonstrate the dependence of the output polarisation ellipticity on that of the pump and that a large degree of circular polarisation can be achieved for the circular pump polarisation. The instability of the 1300 nm spin-VCSEL has been investigated and presented in 2D contour maps.

5 Acknowledgments

The authors thank K. Schires of the University of Essex for fruitful discussions and advice on the spin-VCSELs. This work was supported by the U.K. Engineering and Physical Sciences Research Council (EPSRC) under grant reference EP/G012458/1.

6 References

1 Gerhardt, N., Hofmann, M.: 'Spin-controlled vertical-cavity surface-emitting lasers', *Adv. Opt. Technol.*, 2012, **2012**, p. 268949
2 Sinova, J., Zutic, I.: 'New moves of the spintronics tango', *Nat. Mater.*, 2012, **11**, pp. 368–371
3 Basu, D., Saha, D., Wu, C.C., Holub, M., Mi, Z., Bhattacharya, P.: 'Electrically injected InAs/GaAs quantum dot spin laser operating at 200 K', *Appl. Phys. Lett.*, 2008, **92**, (9), p. 091119
4 Iba, S., Koh, S., Ikeda, K., Kawaguchi, H.: 'Room temperature circularly polarized lasing in an optically spin injected vertical-cavity surface-emitting laser with (110) GaAs quantum wells', *Appl. Phys. Lett.*, 2011, **98**, (8), p. 081113
5 Schires, K., Al Seyab, R., Hurtado, A., *et al.*: 'Optically-pumped dilute nitride spin-VCSEL', *Opt. Express*, 2012, **20**, (4), pp. 3550–3555
6 Schires, K., Al Seyab, R., Hurtado, A., *et al.*: 'Instabilities in optically pumped 1300 nm dilute nitride spin-VCSELs: experiment and theory'. IEEE Photonics Conf. (IPC), San Francisco, USA, 23–27 September 2012, pp. 870–871
7 Rudolph, J., Döhrmann, S., Hägele, D., Oestreich, M., Stolz, W.: 'Room-temperature threshold reduction in vertical-cavity surface-emitting lasers by injection of spin-polarized electrons', *Appl. Phys. Lett.*, 2005, **87**, p. 241117
8 Gerhardt, N., Hövel, S., Hofmann, M., Yang, J., Reuter, D., Wieck, A.: 'Enhancement of spin information with vertical cavity surface emitting lasers', *Electron. Lett.*, 2006, **42**, (2), pp. 88–89
9 Hövel, S., Bischoff, A., Gerhardt, N.C., *et al.*: 'Optical spin manipulation of electrically pumped vertical-cavity surface-emitting lasers', *Appl. Phys. Lett.*, 2008, **92**, p. 041118
10 Gerhardt, N.C., Li, M.Y., Jahme, H., Hopfner, H., Ackemann, T., Hofmann, M.R.: 'Ultrafast spin-induced polarization oscillations with tunable lifetime in vertical-cavity surface-emitting lasers', *Appl. Phys. Lett.*, 2011, **99**, (15), pp. 151107–151107–3
11 Li, M.Y., Jahme, H., Soldat, H., Gerhardt, N.C., Hofmann, M.R., Ackemann, T.: 'Birefringence controlled room temperature picosecond spin dynamics close to the threshold of vertical-cavity surface-emitting laser devices', *Appl. Phys. Lett.*, 2010, **97**, (19), p. 191114
12 Gerhardt, N.C., Li, M.Y., Jahme, H., Soldat, H., Hofmann, M.R., Ackemann, T.: 'Ultrafast circular polarization oscillations in spin-polarized vertical-cavity surface-emitting laser devices'. Proc. SPIE, 2010, vol. 7597, no. 1, pp. 75970Q–1–9
13 Ackemann, T., Sondermann, M.: 'Characteristics of polarization switching from the low to the high frequency mode in vertical-cavity surface-emitting lasers', *Appl. Phys. Lett.*, 2001, **78**, p. 3574
14 Sondermann, M., Ackemann, T., Balle, S., Mulet, J., Panajotov, K.: 'Experimental and theoretical investigations on elliptically polarized

doi: 10.1049/iet-opt.2013.0044

dynamical transition states in the polarization switching of vertical-cavity surface-emitting lasers', *Opt. Commun.*, 2004, **235**, pp. 421–434
15 Gahl, A., Balle, S., Miguel, M.S.: 'Polarization dynamics of optically pumped VCSELs', *IEEE J. Quantum Electron.*, 1999, **35**, (3), pp. 342–351
16 Jouhti, T., Okhotnikov, O., Konttinen, J., *et al*.: 'Dilute nitride vertical-cavity surface-emitting lasers', *New J. Phys.*, 2003, **5**, pp. 84.1–84.6
17 Lombez, L., Braun, P.F., Carrère, H., *et al*.: 'Spin dynamics in dilute nitride semiconductors at room temperature', *Appl. Phys. Lett.*, 2005, **87**, p. 252115
18 Reith, C., White, S.J., Mazilu, M., *et al*.: 'Room temperature electron spin relaxation in GaInNAs multiple quantum wells at 1.3 μm', *Appl. Phys. Lett.*, 2006, **89**, p. 211122
19 Miguel, M.S., Feng, Q., Moloney, J.V.: 'Light-polarization dynamics in surface-emitting semiconductor lasers', *Phys. Rev. A*, 1995, **52**, (2), pp. 1728–39
20 Martin.-Regalado, J., Prati, F., Miguel, M.S., Abraham, N.B.: 'Polarization properties of vertical cavity surface emitting lasers', *IEEE J. Quantum Electron.*, 1997, **33**, (5), pp. 765–783
21 Al-Seyab, R., Alexandropoulos, D., Henning, I.D., Adams, M.J.: 'Instabilities in spin-polarized vertical-cavity surface-emitting lasers', *IEEE Photonics J.*, 2011, **3**, (5), pp. 799–809
22 Al-Seyab, R., Schires, K., Khan, N., Hurtado, A., Henning, I.D., Adams, M.J.: 'Dynamics of polarized optical injection 1550 nm-VCSELs: theory and experiments', *IEEE J. Sel. Top. Quantum Electron.*, 2011, **17**, (5), pp. 1242–1249
23 Hovel, S., Gerhardt, N.C., Brenner, C., *et al*.: 'Spin-controlled LEDs and VCSELs', *Phys. Status Solidi A*, 2007, **204**, (2), pp. 500–507
24 Willemsen, M.B., Van Exter, M.P., Woerdman, J.P.: 'Anatomy of a polarization switch of a vertical-cavity semiconductor laser', *Phys. Rev. Lett.*, 2000, **84**, pp. 4337–4340

doi: 10.1049/iet-opt.2013.0044